Received April 23, 2019, accepted May 18, 2019, date of publication May 22, 2019, date of current version June 4, 2019.

Digital Object Identifier 10.1109/ACCESS.2019.2918231

A 1-Bit Electronically Reconfigurable Reflectarray Antenna in X Band

HAI ZHANG, XUXIANG CHEN, (Student Member, IEEE), ZHENGLONG WANG, YUEHE GE, (Member, IEEE), AND JIXIONG PU

College of Information Science and Engineering, Huaqiao University, Xiamen 361021, China

Corresponding author: Yuehe Ge (yuehe@ieee.org)

This work was supported in part by the National Natural Science Foundation of China (NSFC) under Grant 11674111, Grant 61575070, and Grant 11750110426, in part by the Natural Science Foundation of Fujian Province, China, under Grant 2017J01003 and Grant 2017J01115, in part by the Foreign Cooperation Projects in Fujian Province, China, under Grant 2016I0008, in part by the Foreign Cooperation Projects of Quanzhou City Science and Technology Program of China under Grant 2017T005, and in part by the Subsidized Projects for Postgraduates' Innovative Fund in Scientific Research of Huaqiao University under Grant 1511301030 and Grant 17013082024.

ABSTRACT In this paper, a fully electronically reconfigurable reflectarray antenna that has 14×14 reflecting elements and features a higher aperture efficiency was designed, fabricated, and tested. A new configuration of the reflecting element was first developed so that all the bias circuit and the PIN diode are arranged on the opposite side of the reflecting surface, avoiding the potential unexpected reflection and aiming at the improvement of the antenna efficiency. The new reflecting element, which has a smaller size (0.365λ), was then applied to the design of a 14×14 reconfigurable reflectarray antenna. A field programmable gate array (FPGA)-based beam control system was also developed for the realization of an electronically beam-scanning performance. The measurements of the prototype of the integrated reconfigurable reflectarray antenna show good beam-scanning radiation performance, a peak gain of 19.2 dBi, and an aperture efficiency of about 25%.

INDEX TERMS Reflectarray antenna, reconfigurable antenna, beam-scanning, PIN diode.

I. INTRODUCTION

Reflectarray antennas [1]–[3] are exciting high-gain antennas that exhibit many advantages over their parabolic counterparts, such as low profile, ease of manufacturing, low fabrication cost and the possibilities of beam forming and scanning. Recently, much effort has been made to study the electronically reconfigurable reflectarrays [4]–[17] and transmitarrays [18]–[21], which not only possess the advantages mentioned above, but also provide flexibly scanning beams without using the complicated and high-cost feeding networks.

Electronically reconfigurable reflectarrays carry out the functionalities of beam scanning and beamforming by changing the reflection phase of each element on reflectarrays through controlling active devices. Examples of such active devices include liquid crystal materials [4], [5], varactor diodes [6], [7], [18], RF-MEMS technology [8]–[10], PIN diodes [12]–[17], [19]–[21], etc.. In [4], the main beam is able to steer to $\pm$ 6° by using the liquid crystal, which may not be enough for most beam steering antennas. The phase tuning ability of the varactor is much more powerful. Nearly 360° phase range was achieved by loading a varactor diode with the patch [7]. However, the unit cell has a high insertion loss of 3.7 dB. To solve this problem, amplifiers were integrated with the unit cell, but this would result in increased complexity [7]. In addition, the narrow bandwidths for the unit cells reported in [4]–[7], [18] also limited their applications. Recently, phase reconfigurable unit cells based on PIN diodes have been well developed with the reduced phase resolution (1-bit, typically) [12]–[15], [17], [19]–[21]. In these designs, including both reconfigurable reflectarrays and transmitarrays, the beam-scanning performance based on the 1-bit phase changes has been experimentally demonstrated and studied. It is found that all the 1-bit reconfigurable antenna arrays in literatures have low aperture efficiencies.

In this paper, we present a new configuration of the 1-bit phase-reconfigurable unit cell for reconfigurable reflectarray antennas, which uses only one PIN diode placed on the opposite side of the reflection surface. In the current reconfigurable reflectarray antennas [9]–[16], the PIN diodes and the solders appear on the reflection surface of

The associate editor coordinating the review of this manuscript and approving it for publication was Mohsen Khalily.

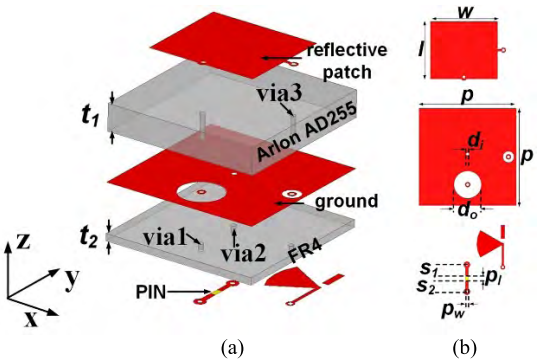

FIGURE 1. Geometry of the unit cell: (a) Schematic 3-D view; (b) Layout of top, middle and bottom layers.

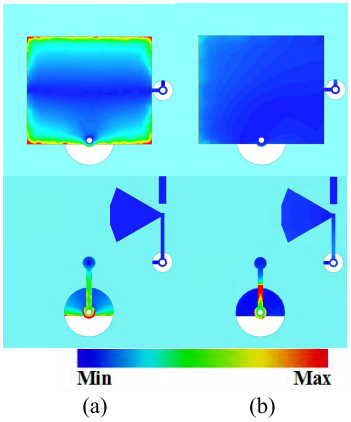

FIGURE 2. Electric field distributions on the top and bottom layers: (a) "ON" state; (b) "OFF" state.

reflectarrays, which might lead to undesirable scattering and hence deteriorate the radiation performance of reflectarrays. In our new design, the PIN diodes, other passive and active lumped devices and the associated solders are arranged not to appear on the reflection surface of reflectarrays. In addition, the proposed unit cell has a smaller size, only 0.365λ, while those in [12]–[15] are greater than or equal to 0.5λ. It is expected that low loss is achieved regardless of the states of the PIN diode and a higher aperture efficiency can be obtained. Simulations and measurements are first conducted to validate the proposed unit cell design. A 14 × 14 reconfigurable reflectarray antenna was then developed for the study of the beam-scanning radiation performance. In order to comprehensively investigate the performance of the new beam-scanning antenna, a field programmable gate array (FPGA)-based beam controller was also developed. The antenna prototype is fabricated and tested. This paper is organized as follows. Section II introduces the new configuration of the 1-bit unit cell and the simulated and experimental characterization results. Section III describes the designs of the 14 × 14 reflectarray antenna and the beam controller, as well as simulation results of the reflectarray antenna. The fabrication and the measured beam-scanning performance of the antenna prototype and the discussion of the experimental results are presented in Section IV. Section V summarizes this paper.

II. REFLECTARRAY ELEMENT DESIGN AND CHARACTERIZATION

A. UNIT CELL DESIGN

The configuration of the proposed 1-bit reflecting element is schematically illustrated in Fig. 1. It consists of two stacked dielectric layers, a rectangular metallic patch ($w \times l$) printed on the top surface of the upper layer, a perfect electric conductor (PEC) ground between the two layers and a grounded line and a biasing circuit as well as a PIN diode on the bottom surface of the lower layer. The two dielectric layers, which have no air gap in between, use Arlon AD255 ($\varepsilon_r = 2.55$, $tan\delta = 0.0014$) and FR4 ($\varepsilon_r = 4.40$, $tan\delta = 0.02$) substrates, respectively. The patch is connected to one end of the ground line through a metallic via, which is isolated from the PEC ground. The other end of the line is connected to the PEC ground through a metallic blind via near the middle of the element. There is a gap in the middle of the line where locates the selected PIN diode. The diode should have a small size and a low insertion loss at the operating frequency, 12 GHz. The M/ACOM PIN diode, MA4AGFCP910, is used in this work. In simulations, the PIN diode is modelled as a lumped resistance with the typical value of 5.2 Ω for forward bias ("ON" state), while for reverse bias ("OFF" state), it acts as a lumped capacitance with the typical value of 18 fF.

The reflection patch on the reflecting element acts as a scatterer controlling the polarization of the reflection wave and affecting the reflection phase. The PIN diode is used to connect the PEC ground to the patch through the grounded line and two vias. By controlling the operating states of the PIN diode, namely "ON" and "OFF" states, the patch will be connected and disconnected to the ground, respectively, resulting in different reflection performance of the reflecting element [13]–[15]. It is expected that nearly unity reflection amplitude for both states whilst a 180° phase difference between them can be achieved. In order to drive the PIN diode to change the reflection phase of the unit cell while minimizing its influence on the reflection amplitude, it is necessary to design a proper dc-biasing network. The biasing circuit has to be designed in such a way that the biasing point should be placed at the position with the electric field of nearly zero. A quarter-wavelength microstrip line with an open-ended radial stub is considered [14], [15] to isolate the RF signal from the dc signal. Fig. 2 shows the electric field distributions on the surfaces of top and bottom layers for both "on" and "off" states under the y-polarized incident wave. It can be seen that the amplitude of the electric field on the position of the biasing line, where the open-ended radial stub is connected, is nearly zero. While the PIN diode in this design is mounted on the bottom of the layer, which avoids the scattering resulting from the PIN diode and the solders, the operating principle of the unit cell is similar to those of [14], [15], which is that by changing the state of the PIN diode into "ON" or "OFF", the resonant frequencies

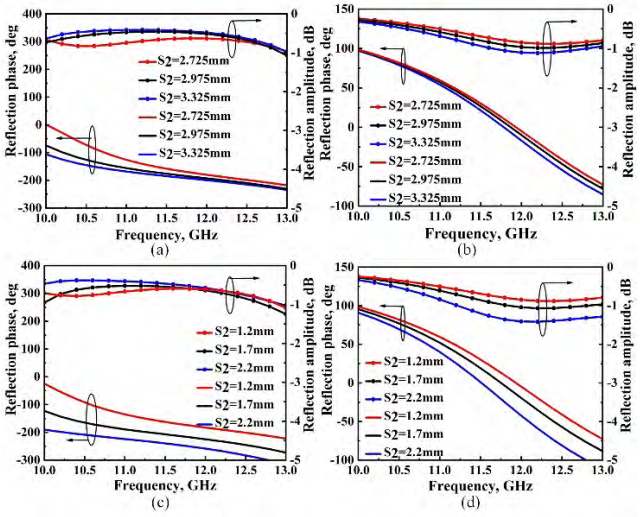

FIGURE 3. Reflection amplitudes and phases with different positions of the vias and the PIN diode: (a) via2 and the PIN diode are fixed, via1 is varied and the Pin diode is at "OFF" state; (b) via2 and the PIN diode are fixed, via1 is varied and the Pin diode is at "ON" state; (c) via1 is fixed, via2 and the PIN diode are varied and Pin diode is at "OFF" state; (d) via1 is fixed, via2 and the PIN diode are varied and Pin diode is at "ON" state.

of the reflecting unit cell are different, resulting in different reflection phases. The size of the unit cell is also smaller, only $0.365\lambda \times 0.365\lambda$, while the counterparts in [14], [15] are both $0.5\lambda \times 0.5\lambda$. The corresponding geometry parameters of the final design, shown in Fig. 1, are as follows: $p = 9.525$ mm, $w = 5.85$ mm, $l = 6.8$ mm, $t_1 = 1.58$ mm, $t_2 = 0.5$ mm, $d_i = 0.3$ mm, $d_o = 2.2$ mm, $s_1 = 1.2$ mm, $s_2 = 1.2$ mm, $p_l = 0.3$ mm, and $p_w = 0.3$ mm.

B. SIMULATED AND EXPERIMENTAL CHARACTERIZATION

We carried out numerical simulations by using the commercial full-wave EM software Ansys HFSS. The effects of the positions of via1, via2 and the PIN diode on the reflection amplitude and phase are first studied. Fig. 3 shows the results. As can be seen, the reflection amplitude and phase are more or less affected by the positions of the vias and the PIN diode. The final results with parameters above are plotted in Fig. 4. It is observed that the phase difference (δ) between the "ON" and "OFF" states is very close to 180° from 10.9 to 12.1 GHz, indicating that the required binary reconfigurable phases are successfully obtained. Furthermore, there is no remarkable difference between the two reflection amplitudes, which are both above −0.7 dB, regardless of the PIN diode states.

For experimental verification, several identical samples are fabricated and measured using a waveguide simulator (WGS) [22], [23]. The front and back views of the prototypes are shown in Fig. 5(a). The sample consists of three identical elements. In order to avoid the propagation of substrate modes outside the elements, a rectangular ring formed by metallic vias is made surrounding the three elements. The test system is composed of a coax-to-WR75

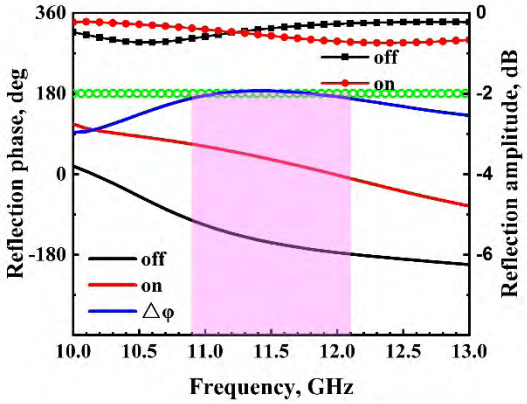

FIGURE 4. Simulated reflection phase and amplitude of the proposed element under the normal incidence.

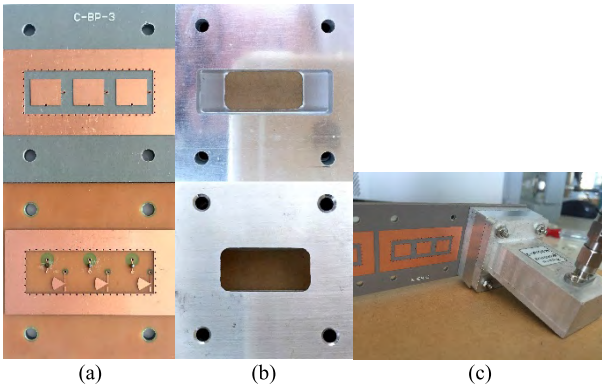

FIGURE 5. Photographs of the fabricated samples and measurement setup: (a) Three identical elements; (b) Transition; (c) Measurement setup.

adaptor and a WR75 waveguide. In addition, the measurement setup also includes a transition between the WR75 waveguide (9.525 mm × 19.05 mm) and the three unit cells (9.525 mm × 28.575 mm) due to their different dimensions, as shown in Fig. 5(b). The reflecting elements under measurement are shown in Fig. 5(c). In the WGS, all the walls of the waveguide are perfect conductors. In order to characterize an element of an array, the oblique incidence should be applied in the E-plane of the element, as detailed in [22], [23].

Fig. 6 shows the comparisons between the simulated results using periodic boundary conditions (PBCs) under the normal incidence and the WGS results from both simulations and experiments. The agreements of reflection phases among the three cases are good and all the three phase differences within the frequency range of 11-12 GHz are in the range of 180°−200°. Although the reflection amplitudes show slight differences, they are all above −1 dB at 11-12 GHz. These slight differences are attributed to the fabrication tolerance and assembly misalignment among the waveguide, the transition and the fabricated sample. In summary, these results demonstrate that the proposed design is capable of forming 1-bit reconfigurable reflectarray antennas, developed in the next section.

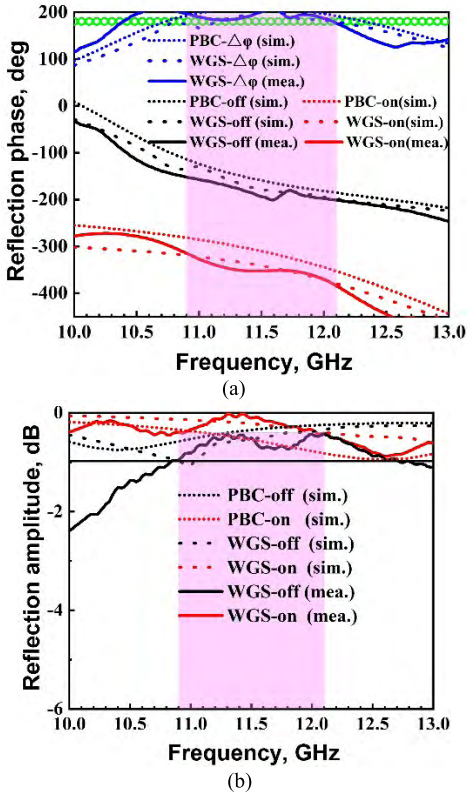

FIGURE 6. Comparison between simulated and measured reflection performance: (a) Phases; (b) Amplitudes.

III. RECONFIGURABLE REFLECTARRAY ANTENNA

After the successful design of the reflecting element, a 1-bit reconfigurable reflectarray consisting of 14 × 14 elements was designed. The schematic reconfigurable reflectarray antenna, shown in Fig. 7, is composed of a feed, a reflectarray and a beam-scanning controller. The incident wave from the feed horn illuminates the reflectarray. The reflection phases of all elements on the reflectarray are only 0° or 180°, which are controlled by the beam-scanning controller. In order to realize radiation patterns with required main beam directions or shaped beams, the appropriate design considerations of the antennas are required, as follows.

A. REFLECTARRAY DESIGN

The common methods to design planar reflectarrays include Fresnel zone principle and the phase compensation method. The latter ideally needs continuous compensation phases over 0°−360°. However, discrete phases are used in practice, resulting in the reduction of the radiation performance of reflectarrays, such as the gain, the sidelobe level, the beam direction errors, etc.. In this work, the compensation phases are only 0° and 180°, which are the minimum requirement for the phase compensation method. It is well known that the radiation performance of reflectarray antennas using such kind of phase compensation would be improved with the increase of the antenna size, namely, the more elements the reflectarray has the better the radiation performance

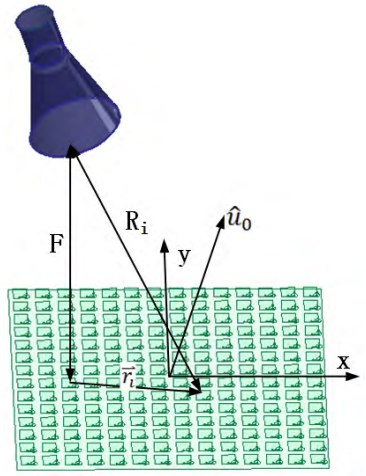

FIGURE 7. Schematic reconfigurable reflectarray antenna and the coordinate system.

is [14], [15]. In our design, a reflectarray with 14 × 14 elements is considered.

Fig. 7 shows the schematic geometry of the reconfigurable reflectarray antenna, where F is the focusing distance between the phase center of the feed and the reflectarray, R_i is the distance between the feed and the i^{th} element on the reflectarray, $\vec{r}_i$ is the position vector of the i^{th} element, and $\hat{u}_0$ is the unit vector of the main beam direction. The required compensation phase of each element can be obtained using the following equation [1]

$$\varphi_i = k\left(R_i - F + \vec{r}_i \cdot \hat{u}_0\right) \mp 2n\pi + \varphi_0 \tag{1}$$

where φ_i and φ_0 are the compensation phases of the i^{th} and the center elements of the reflectarray respectively, k is the propagation constant, and n is an integer number to make sure that $0 < \varphi_i < 360°$. In our design, the compensation phase will be 0° when $-90° < \varphi_i < 90°$ and 180° for other φ_i.

B. FEED

Normally the illumination at the reflectarray edge from the feed is about −10 dB [1]. In order to appropriately illuminate the reflectarray, a conical horn antenna that has a gain of around 15 dBi at 12 GHz is first developed. Due to the limited reflectarray aperture size, which is 134 × 134 mm^2, −9 dB illumination at the reflectarray edge is applied and hence the focusing length of the feed horn is 189 mm. The phase center of the horn is about 7.4 mm below the horn aperture. Therefore, the length between the horn aperture and the surface of the reflectarray is 181.6 mm. In addition, in order to avoid the blockage of the feed when the antenna beam is scanning, the offset feed is necessary. In our design, the feed horn is located in the XOZ plane and the offset angle is 17.5°.

C. SIMULATIONS

The reconfigurable reflectarray antenna design is first simulated to evaluate its potential performance. Commercial softwave Ansys HFSS is applied to carry out simulations.

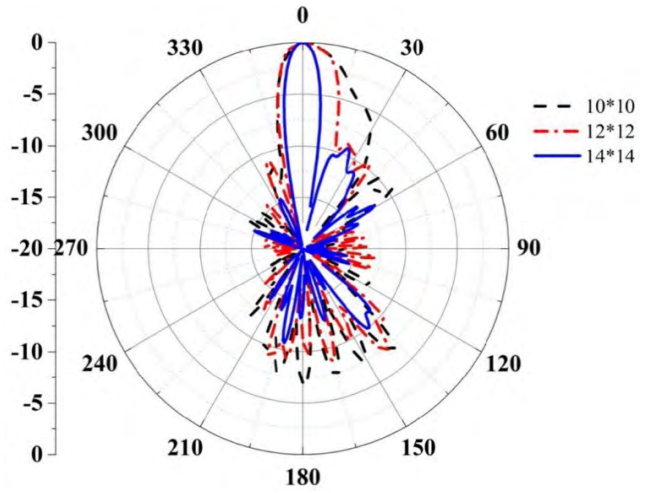

FIGURE 8. Simulated radiation patterns at 11.5 GHz for three reflectarrays with different sizes.

In our simulations, the exactly same reflecting element and horn models, as shown in Fig. 1 and designed in Section III-B, are applied to form the reflectarray antenna models. Therefore, the phase change for each element on the reflectarray, according to the requirements of the beam scanning, will be carried out by changing the ''ON'' and ''OFF'' states of the diode on the element.

The radiation performance for reflectarrays with different sizes are first simulated. Reflectarrays with 10×10, 12×12, and 14×14 elements are respectively applied. Fig. 8 shows the simulated radiation patterns with main beam direction of $(\theta = 0°, \varphi = 0°)$ at 11.5 GHz. As predicted, the performance of the main beam, the sidelobe level and the backlobe level are improved with the increase of the reflectarray size. It can be seen that the reflectarray with 14×14 elements gives reasonable radiation pattern whereas the other two cases result in some distortion in the main beam and high-level sidelobes and backlobes. Hence, the reflectarray with 14×14 elements is applied to the design in this work.

Next, the radiation patterns with the main beam directions from $-30°$ to $60°$ with a $10°$ step are simulated in the XOZ plane at 11.5 GHz. The phase distributions on the 14×14 reflectarray elements for different main beam directions are obtained using formula (1). Fig. 9(a) plots the phase and diode state distributions for the main beams of $-10°$ and $10°$ in the XOZ plane. The simulated radiation patterns are depicted in Fig. 9(b). Due to the blockage of the feed, which is also in the XOZ plane, the radiation patterns with main beam directions of $-30°$, $-20°$ and $-10°$ have the relatively larger sidelobe levels while the performance of those with main beam directions greater than $40°$ will deteriorate because the beamwidths become wider and distortion. The simulated performance confirms to the prediction and demonstrates the validation of the antenna design. The best gain appears when the main beam direction is $10°$ in the XOZ plane, which is about 20 dBi and the corresponding aperture efficiency is 30.45%.

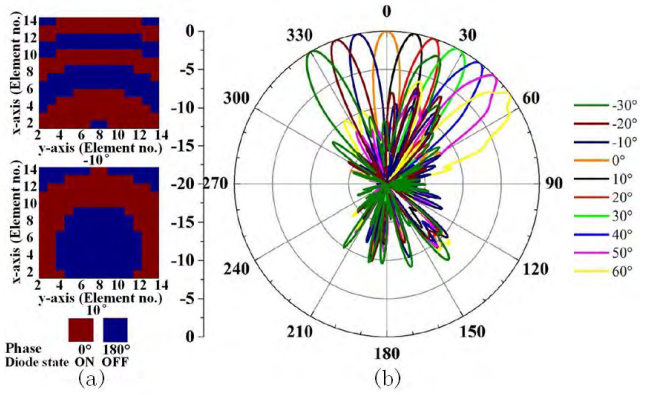

FIGURE 9. (a) Phase distributions for main beams of $-10°$ and $10°$ respectively; (b) The simulated scanning radiation patterns from $-30°$ to $60°$ with a $10°$ step at 11.5 GHz in the XOZ plane.

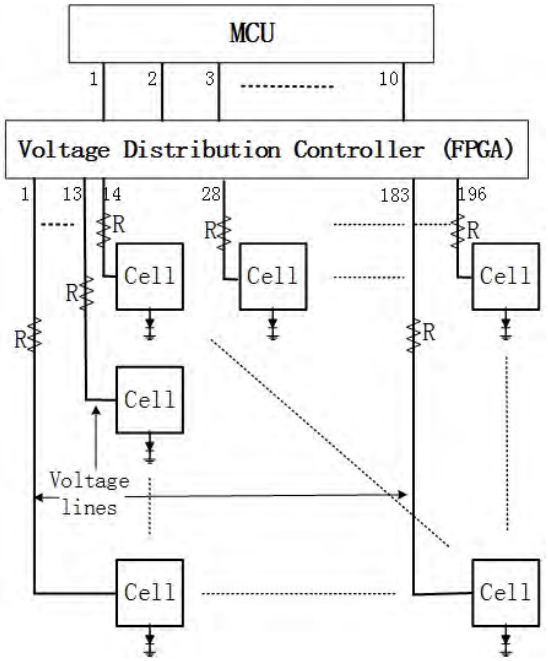

FIGURE 10. Beam control circuitry of the reflectarray.

D. BEAM-SCANNING CONTROLLER

In order to carry out the beam scanning performance and control the main beam direction, a beam controller is developed to control the diode states of each element on the reflectarray. Since each element is controlled by a PIN diode, total 196 PIN diodes and the equivalent number of biasing lines are needed to control the entire reflectarray. The schematic control circuitry is illustrated in Fig. 10, which is mainly composed of a micro-controller-unit (MCU) and a voltage distribution controller (VDC). The VDC has ten inputs and 196 outputs. The outputs are voltages, applied to the diodes of elements on the reflectarray through biasing lines and used to control the ''ON'' and ''OFF'' states of diodes. The ten inputs are used to control the 196 outputs. Each input has

either "0" or "1" state. Therefore, the 10-bit inputs are able to totally control (or select) 1024 (2^{10}) different groups of outputs, corresponding to 1024 different radiation beams.

In our beam control system, the VDC was implemented using the voltage control circuit based on a field programmable gate array (FPGA), which is based on Cyclone IV series chips. The supply voltage of the circuit board is 5V while the output voltage of each output is either 0 V or 3.3 V. Due to the operating voltage 1.33V of the PIN diodes, a series resistor R is needed in each biasing line, as shown in Fig. 10.

Each scanning beam of the reconfigurable reflectarray antenna corresponds to a phase distribution on the 14 × 14 reflection elements, which is realized by a group of 196 outputs of the VDC. All phase distributions of the designated beams can be determined in advance, using formula (1). Therefore, all the corresponding groups of 196 outputs can be estimated and stored in advance in the FPGA based beam control system. The required beams can be selected by the 10-bit digit inputs controlled by the MCU.

IV. EXPERIMENTAL RESULTS AND DISCUSSION

A. REFLECTARRAY PROTOTYPE

In order to experimentally validate the reconfigurable reflectarray antenna design in this work, an antenna prototype, including the feed horn, the reflectarray and the beam controller, are fabricated. Arlon AD255 and FR4 substrates, with thicknesses of 1.58 mm and 0.5 mm respectively, are applied to the fabrication of the reflectarray, which includes 14 × 14 elements and has a surface size of 134 × 134 mm^2. The normal PCB techniques are applied to the fabrication of the reflectarray and the beam controller. Since there is no gap between the two substrates of the reflectarray, an ultrathin FR4 PP sheet is used to agglutinate the two substrates. The total thickness of the reflactarray board is less than 2.1 mm. Fig. 11 shows the mounted antenna prototype. It can be seen that there are only square metallic patches on the reflection surface of the reflactarray. All the diodes, series resistors, and biasing lines are located on the surface of the FR4 substrate, opposite side of the reflectarray. The beam controller board is mounted below the reflectarray, as shown in Fig. 11. The outputs of the VDC are connected to the biasing lines using the normal flat ribbon cables.

B. RADIATION PERFORMANCE

The mounted reflectarray antenna, shown in Fig. 11, was measured using a far-field testing system in an anechoic chamber. The radiation performance in the XOZ plane, where the feed horn is located, is first measured at 11.5 GHz. The measured radiation patterns with main beam directions from −30° to 60°, stepped by 10°, were plotted in Fig. 12. Due to the blockage of the feed, the patterns with the main beam close to the position of the feed, such as −30°, −20°, −10°, and 0°, have high-level sidelobes and abnormal half-power beamwidths (HPBW), which are different than simulated ones in Fig. 9. The main reason is

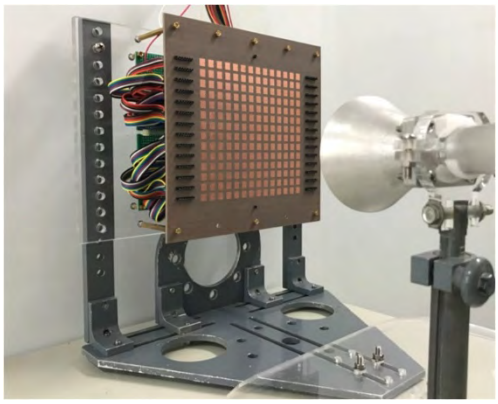

FIGURE 11. Fabricated reflectarray antenna prototype.

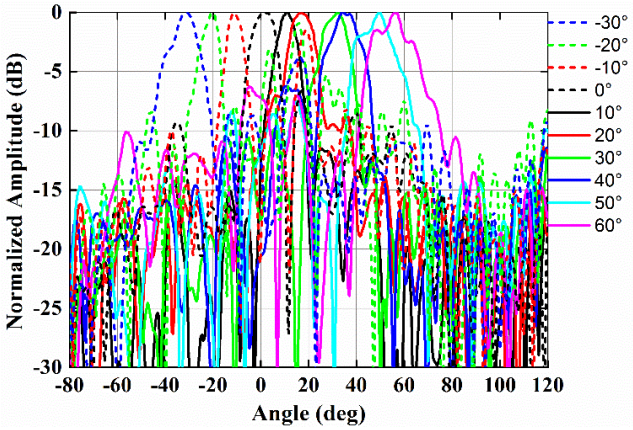

FIGURE 12. Measured radiation patterns for the main beam scanned from −30° to 60° with a step of 10° in the XOZ plane at 11.5 GHz.

contributed that the position of the feed horn in measurements is slightly deviated from the determined place due to the misalignment during the antenna mounting and the deviation during the rotation of the antenna under measurements. The offset angle might change due to the aforementioned reasons in the measurements. During the measurement of each beam, the receiving signal amplitudes are automatically normalized to the maxima by the measurement software. Therefore, the gain reduction cannot be plotted in Fig. 12. In addition, with the increase of the scanning angle, the sidelobe levels and the main beams also deteriorate. The main reason is that the reduction of the reflection amplitudes and the phase errors from the reflectarray elements will increase with the scanning angle. Table 1 lists the measured beam direction errors and the HPBW for each scanning beam. The measured gains and aperture efficiencies for different scanning beams in the XOZ plane at 11.5 GHz are also measured and depicted in Fig. 13, together with simulated ones for comparison. The measured peak gain appears at the 10° main beam, about 19.2 dB. The corresponding peak aperture efficiency is about 25%. Due to the blockage of the feed and the tolerance when mounting the feed horn, the gain drops a lot when the beam scanning angle is close to the direction of the feed.

TABLE 1. Measured beam direction errors and HPBW under different beam directions at 11.5 GHz in the XOZ plane.

Scan angle	Direction error	HPBW
0°	1.46°	11.4°
-10°/10°	0.83°/0.67°	11.4°/9.2°
-20°/20°	0.43°/1.73°	8.19°/11.6°
-30°/30°	0.6°/1.47°	7.4°/11.8°
40°	2.53°	14.8°
50°	0.02°	16.8°
60°	2.93°	18.8°

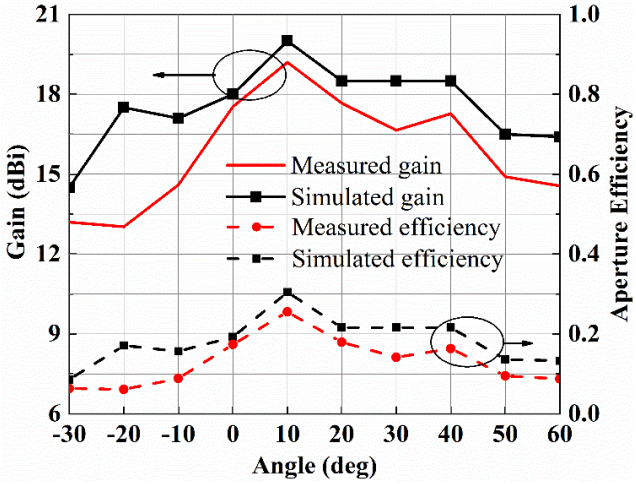

FIGURE 13. The measured and simulated gains and aperture efficiencies for different scanning beams in the XOZ plane at 11.5 GHz.

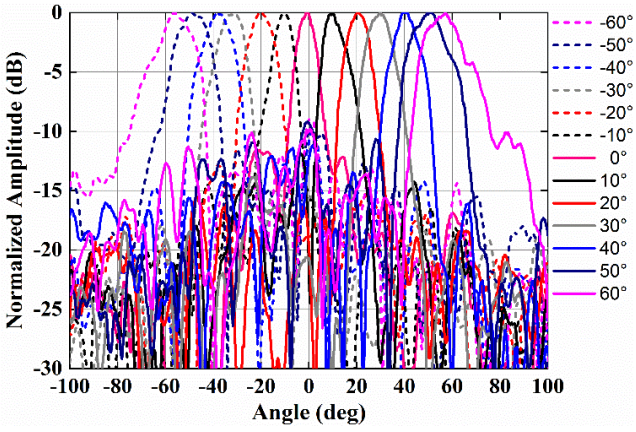

FIGURE 14. Measured radiation patterns for main beams scanned from −60° to 60° with a step of 10° in the YOZ plane at 11.5 GHz.

The radiation performance in the YOZ plane at 11.5 GHz is also measured. In the measurement, the beam scans from −60° to 60°, with a step of 10°. Fig. 14 and 15 plot the measured radiation patterns, the gains and the aperture efficiencies respectively. Same as those in the XOZ plane, the radiation performance deteriorate when the scanning angles are greater than 40°. Since there is no blockage in the YOZ plane, the sidelobe levels are much better than those

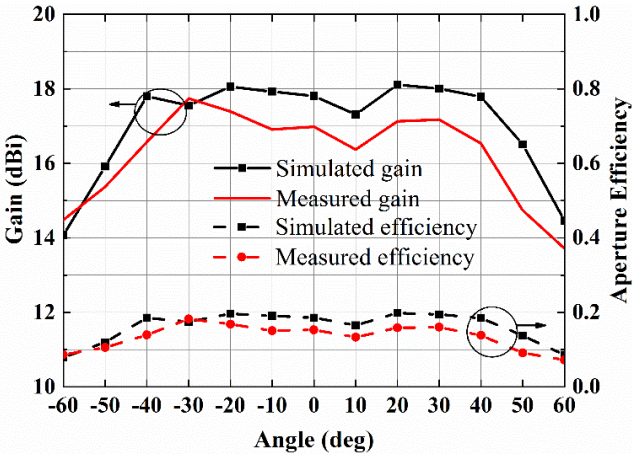

FIGURE 15. The measured and simulated gains and aperture efficiencies for different scanning beams in the YOZ plane at 11.5 GHz.

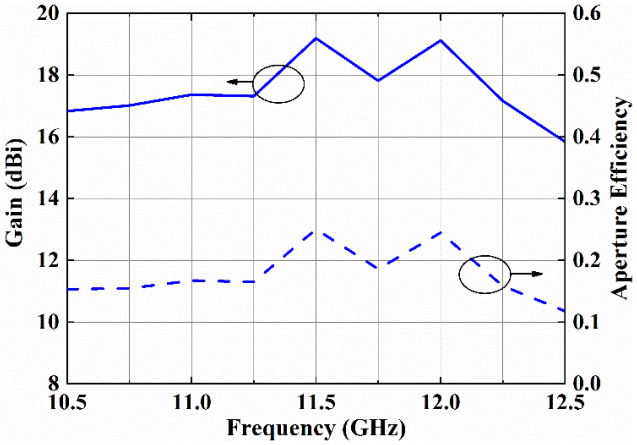

FIGURE 16. Measured gain and aperture efficiency curves for the main beam fixed at 10° in the XOZ plane.

in the XOZ plane, the beam direction errors are much less, and the gains do not drop significantly with the increase of scanning angles. The radiation performance for different frequencies is also tested. Fig. 16 shows the measured gain and efficiency curves for the main beam fixed at 10° ($\theta = 10°, \varphi = 0°$) in the XOZ plane.

Table 2 compares the performance, the size and the working modes of the proposed antenna to those reported in literatures. It is shown that the proposed 1-bit reconfigurable reflectarray antenna design features a higher aperture efficiency, achieving the main target of this work.

C. DISCUSSION

Overall, the experimental results successfully demonstrate the beam-scanning radiation performance of the reconfigurable reflectarray antenna design, validating the reflecting element design in Section II. Nevertheless, the radiation performance deteriorates with the increase of the scanning angle. The gain drops a lot and the HPBW distorts much. The main reasons include the feed blockage, the substrate

TABLE 2. Comparison of different reconfigurable antenna arrays.

	Ref.[12]	Ref.[14]	Ref.[15]	Ref.[19]	This work
Freq.	60 GHz	12.5 GHz	11.1GHz/ 14.3GHz	9.8 GHz	11.5GHz
Working mode	Refl.	Refl.	Refl.	Trans.	Refl.
No. of elements	160× 160	10×10	40×40	20×20	14×14
Size	114λ× 114λ	5λ×5λ	20λ×20λ	10λ×10λ	5.1λ× 5.1λ
Scanning range	-20° ~ +20°	-50° ~ +50°	-60° ~ +60°	-70° ~ +70°	-60° ~ +60°
Peak gain	42 dBi	17.5 dBi	29.3dBi/ 30.8dBi	22.7dBi	19.2dBi
Aperture efficiency	9.5%	17.9%	21.5%/ 18.1%	15.43%	25.33%

tolerance and the fabrication tolerance, as well as the mounting tolerance of the feed and the measurement tolerance due to the misalignment of the antenna during measurements. In addition, due to the laboratory condition, all the diodes and resistors are soldered manually. The non-uniform solders in different elements might slightly affect their performance. Above all is the size of the reflectarray. As mentioned in Section III and demonstrated in [14], [15], the radiation performance of such kind of reconfigurable reflectarray antennas will become better and the performance deterioration with the increase of the scanning angle will mitigate when the reflectarray size is large enough.

In spite of all these, it should be noted that the measured peak aperture efficiency is about 25%. Compared with those in literatures, for example, 17.9% in [14] and 21.6% in [15], our results show better aperture efficiency. Note that the reflectarrays in [14], [15] use similar reflecting element, include 10×10 and 40×40 elements respectively, which demonstrate that the aperture efficiency is improved with the increase of the reflectarray aperture size. The main reason for the higher aperture efficiency in our reflectarray design is attributed to the arrangement of the PIN diodes in our element design, the smaller size of the reflectarray element and perhaps the use of Arlon AD255 substrate, which has a minor smaller loss tangent ($\tan\delta = 0.0014$) than Taconic TLX-8 ($\tan\delta = 0.0019$) in [14], [15]. As mentioned in Section I, the main difference between our reflecting element and all others in literatures is that the PIN diode and the associated biasing line and solders are designed to be located in the opposite side of the reflection surface of the element, aiming at the improvement of the antenna efficiency. In addition, although our reflectarray has 14×14 elements while that in [14] has 10×10 elements, the two reflectarrays have similar aperture size, $5.1\lambda \times 5.1\lambda$ and $5\lambda \times 5\lambda$ respectively. The size of the element in our reflectarray design is smaller. With the similar aperture size, the same 1-bit compensation phase while more reflectarray elements, our design exhibits a higher aperture efficiency, illustrating that the negative effect of phase errors on the radiation performance of an 1-bit reconfigurable reflectarray might be mitigated by using elements with a smaller size. Both simulations in Section III-C and experiments in Section IV-B show the realization of our initial target. It is expected that the reconfigurable reflectarray antenna based on our reflecting element is able to achieve better aperture efficiency when with larger aperture sizes.

V. CONCLUSION

We have successfully demonstrated an X-band electronically reconfigurable reflectarray antenna that has 14×14 reflecting elements and features a higher aperture efficiency. A 1-bit electronically controlled reflecting element with only one PIN diode and a smaller period (0.365λ) has been successfully developed for reconfigurable reflectarray antennas. The 180° phase difference is achieved by controlling the ''ON'' and ''OFF'' states of the PIN diode mounted on the opposite side of the reflection surface, with the reflection amplitude of > -1dB. Measurements in a WGS show good agreements with the simulated results, validating the proposed design.

A 14×14 reflectarray, a feed horn and a FPGA based beam controller are further developed to demonstrate the beam-scanning radiation performance. The measured results show a peak gain of 19.2 dBi and an aperture efficiency of 25% at 11.5 GHz, realizing one of the main aims of this work, namely, to improve the antenna efficiency. Good beam-scanning performance is achieved in a 2D space. This antenna is able to be scaled to operate at other frequencies. The potential applications include current and future communication, satellite and radar systems.

REFERENCES

[1] J. Huang and J. A. Encinar, *Reflectarray Antennas*, Piscataway, NY, USA: Wiley, 2008.
[2] Y. Chen, Y. Ge, and T. S. Bird, ''An offset reflectarray antenna for multi-polarization applications,'' *IEEE Antennas Wireless Propag. Lett.*, vol. 15, pp. 1353–1356, 2015.
[3] M. H. Dahri, M. I. Abbasi, M. H. Jamaluddin, and M. R. Kamarudin, ''A review of high gain and high efficiency reflectarrays for 5G communications,'' *IEEE Access*, vol. 6, pp. 5973–5985, 2018.
[4] G. Perez-Palomino, R. Florencio, J. A. Encinar, M. Barba, R. Dickie, R. Cahill, P. Baine, M. Bain, and R. R. Boix, ''Accurate and efficient modeling to calculate the voltage dependence of liquid crystal-based reflectarray cells,'' *IEEE Trans. Antennas Propag.*, vol. 62, no. 5, pp. 2659–2668, May 2014.
[5] S. Bildik, S. Dieter, C. Fritzsch, W. Menzel, and R. Jakoby, ''Reconfigurable folded reflectarray antenna based upon liquid crystal technology,'' *IEEE Trans. Antennas Propag.*, vol. 63, no. 1, pp. 122–132, Jan. 2015.
[6] S. V. Hum, M. Okoniewski, and R. J. Davies, ''Modeling and design of electronically tunable reflectarrays,'' *IEEE Trans. Antennas Propag.*, vol. 55, no. 8, pp. 2200–2210, Aug. 2007.
[7] F. Venneri, S. Costanzo, G. Di Massa, E. Marozzo, A. Borgia, P. Corsonello, and M. Salzano, ''Beam-scanning reflectarray based on a single varactor-tuned element,'' *Int. J. Antennas Propag.*, vol. 2012, Jan. 2012, Art. no. 290285.
[8] H. Rajagopalan, Y. Rahmat-Samii, and W. A. Imbriale, ''RF MEMS actuated reconfigurable reflectarray patch-slot element,'' *IEEE Trans. Antennas Propag.*, vol. 56, no. 12, pp. 3689–3699, Dec. 2008.
[9] E. Carrasco, M. Barba, B. Reig, C. Dieppedale, and J. A. Encinar, ''Characterization of a reflectarray gathered element with electronic control using ohmic RF MEMS and patches aperture-coupled to a delay line,'' *IEEE Trans. Antennas Propag.*, vol. 60, no. 9, pp. 4190–4201, Sep. 2012.

[10] T. Debogovic and J. Perruisseau-Carrier, "Low loss MEMS-reconfigurable 1-bit reflectarray cell with dual-linear polarization," *IEEE Trans. Antennas Propag.*, vol. 62, no. 10, pp. 5055–5060, Oct. 2014.
[11] S. V. Hum and J. Perruisseau-Carrier, "Reconfigurable reflectarrays and array lenses for dynamic antenna beam control: A review," *IEEE Trans. Antennas Propag.*, vol. 62, no. 1, pp. 183–198, Jan. 2014.
[12] H. Kamoda, T. Iwasaki, J. Tsumochi, T. Kuki, and O. Hashimoto, "60-GHz electronically reconfigurable large reflectarray using single-bit phase shifters," *IEEE Trans. Antennas Propag.*, vol. 59, no. 7, pp. 2524–2531, Jul. 2011.
[13] E. Carrasco, M. Barba, and J. A. Encinar, "X-band reflectarray antenna with switching-beam using PIN diodes and gathered elements," *IEEE Trans. Antennas Propag.*, vol. 60, no. 12, pp. 5700–5708, Dec. 2012.
[14] H. Yang, F. Yang, S. Xu, Y. Mao, M. Li, X. Cao, and J. Gao, "A 1-bit 10×10 reconfigurable reflectarray antenna: Design, optimization, and experiment," *IEEE Trans. Antenna Propag*, vol. 64, no. 6, pp. 2246–2254, Jun. 2016.
[15] H. Yang, F. Yang, X. Cao, S. Xu, J. Gao, X. Chen, M. Li, and T. Li, "A 1600-element dual-frequency electronically reconfigurable reflectarray at X/Ku-band," *IEEE Trans. Antennas Propag.*, vol. 65, no. 6, pp. 3024–3032, Jun. 2017.
[16] X. Yang, S. H. Xu, F. Yang, and M. K. Li, "A novel 2-bit reconfigurable reflectarray element for both linear and circular polarizations," in *Proc. IEEE Int. Symp. Antennas Propag. USNC/URSI Nat. Radio Sci. Meeting*, Jul. 2017, pp. 2083–2084.
[17] X. Chen and Y. Ge, "A 14 × 14 electronically reconfigurable reflectarray using 1-bit reflective element," in *IEEE MTT-S Int. Wireless Symp. Dig.*, Chengdu, China, May 2018, pp. 1–3.
[18] W. Pan, C. Huang, X. Ma, and X. Luo, "An amplifying tunable transmitarray element," *IEEE Antennas Wireless Propag. Lett.*, vol. 13, pp. 702–705, 2014.
[19] A. Clemente, L. Dussopt, R. Sauleau, P. Potier, and P. Pouliguen, "Wideband 400-element electronically reconfigurable transmitarray in X band," *IEEE Trans. Antennas Propag.*, vol. 61, no. 10, pp. 5017–5027, Oct. 2013.
[20] M. Wang, S. H. Xu, F. Yang, and M. K. Li, "Design of a Ku-band 1-bit reconfigurable transmitarray with 16 × 16 slot coupled elements," in *Proc. IEEE Int. Symp. Antennas Propag. USNC/URSI Nat. Radio Sci. Meeting*, Jul. 2017, pp. 1991–1992.
[21] L. D. Palma, A. Clemente, L. Dussopt, R. Sauleau, P. Potier, and P. Pouliguen, "Circularly-polarized reconfigurable transmitarray in Ka-band with beam scanning and polarization switching capabilities," *IEEE Trans. Antennas Propag.*, vol. 65, no. 2, pp. 529–540, Feb. 2017.
[22] P. W. Hannan and M. A. Balfour, "Simulation of a phased-array antenna in waveguide," *IEEE Trans. Antennas Propag.*, vol. 13, no. 3, pp. 342–353, May 1965.
[23] N. Lenin and P. H. Rao, "Evaluation of the reflected phase of a patch using waveguide simulator for reflectarray design," *Microw. Opt. Technol. Lett.*, vol. 45, no. 6, pp. 528–531, Jun. 2005.

HAI ZHANG received the B.E. degree in electronic information engineering from Northwest Polytechnical University, in 2003, and the M.E. and Ph.D. degrees in electronic science and technology from Xi'an Jiaotong University, in 2006 and 2010, respectively. Since 2010, he has been with the School of Information Science and Engineering, Huaqiao University. His current research interests involve high power microwave and millimeter-wave techniques, terahertz techniques, plasma physics, and antenna design.

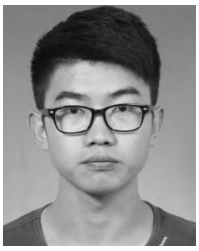

XUXIANG CHEN (S'17) was born in Jiangsu, China, in 1992. He received the B.E. degree in electronic information engineering and the M.E. degree in electromagnetic field and microwave technology from Huaqiao University, Xiamen, China. He is currently an Engineer with Antenna and Subsystems Business Unit, Comba Telecom Systems Ltd., Guangzhou, China. His current research interests include reconfigurable antennas, reflectarrays and transmitarrays, and metasurfaces and its applications.

Mr. Chen received the Honorable Mention Awards of Student Paper Competition at the 2017 IEEE AP-S Symposium on Antennas and Propagation and USNC-URSI Radio Science Meeting (APS 2017) and the 2018 IEEE International Workshop on Antenna Technology: Small Antennas and Innovative Structures.

ZHENGLONG WANG was born in Anhui, China, in 1993. He received the B.E. degree in electronic information engineering from Hefei Normal University, China, in 2017. He is currently pursuing the M.E. degree in electromagnetic field and microwave technology with Huaqiao University, Xiamen, China. His current research interests include reconfigurable antennas, reflectarrays, and transmitarrays.

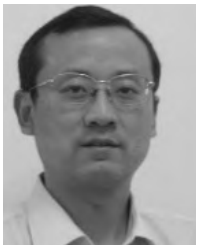

YUEHE GE (S'99–M'02) received the Ph.D. degree in electronic engineering from Macquarie University, Sydney, Australia, in 2003.

From 1991 to 1999, he was an Antenna Engineer with the Nanjing Marine Radar Institute, China. From 2002 to 2011, he was a Research Fellow with the Department of Electronic Engineering, Macquarie University, Australia. Since 2011, he has been a Professor with Huaqiao University, China. His research interests include antenna theory and designs for radar and communication applications, computational electromagnetics and optimization methods, and metamaterials and metasurfaces as well as their applications. He has authored and coauthored over 180 journal and conference publications and two book chapters. He is a member of the IEICE and ACES. He received several prestigious prizes from the China State Shipbuilding Corporation and the China Ship Research and Development Academy, due to his contributions to China State research projects. He has received 2000 IEEE MTT-S Graduate Fellowship Awards and the 2002 Max Symons Memorial Prize of the IEEE NSW Section, Australia, for the Best Student Paper. He is the co-winner of the 2004 Macquarie University Innovation Awards-Invention Disclosure Award. He has served as a Technical Reviewer for over 10 international journals and conferences.

JIXIONG PU received the B.S. degree in physics and the M.S. degree in optics from Fujian Normal University, China, in 1983 and 1986, respectively. Since 1986, he has been a Faculty Member with Huaqiao University, China. He became a Full Professor, in 1999. He visited the University of Tsukuba, Japan, from 1998 to 1999, and as a visiting scholar and JSPS Fellow, from 2001 to 2002. His main research interests are propagation and focusing of laser beams, modulation of the light field, and nonlinear optics.